

RSC Advances



This is an *Accepted Manuscript*, which has been through the Royal Society of Chemistry peer review process and has been accepted for publication.

Accepted Manuscripts are published online shortly after acceptance, before technical editing, formatting and proof reading. Using this free service, authors can make their results available to the community, in citable form, before we publish the edited article. This *Accepted Manuscript* will be replaced by the edited, formatted and paginated article as soon as this is available.

You can find more information about *Accepted Manuscripts* in the [Information for Authors](#).

Please note that technical editing may introduce minor changes to the text and/or graphics, which may alter content. The journal's standard [Terms & Conditions](#) and the [Ethical guidelines](#) still apply. In no event shall the Royal Society of Chemistry be held responsible for any errors or omissions in this *Accepted Manuscript* or any consequences arising from the use of any information it contains.



Effective Segregation of Cytocompatible Chitosan Molecules by Silica-Surfactant Nanostructure formation Process †

Received 00th January 20xx,
Accepted 00th January 20xx

M. Tagaya ^{a, b, *}

DOI: 10.1039/x0xx00000x

www.rsc.org/

Effective segregation of chitosan (Chi) molecules in a silica-surfactant nanostructure formation process was investigated to find the unique self-assembled nanostructures of Chi. The formation process induced the well-defined segregation nanofiber networks to resultantly exhibit the osteoblast-like cell adhesion and spreading, suggesting the unique Chi segregation nanostructures for the cytocompatibility.

The *in vivo* biomineralization processes generating intricate silica-based hierarchical nanostructures are species-specific and attractive.¹ However, the possibility of controlling them remains a long-term major challenge. Recent strong interest raises the supramolecular nanostructured surfaces using a soft self-assembly process, and the surface properties with spatial nanotopological structures are expected to effectively promote the cell adhesion and subsequent functions (e.g., proliferation, differentiation).² Thus, the nanostructured surfaces of biocompatible molecules induced by the self-assemble process have intensively been investigated.³

The supramolecular-templating method using structure-directing agent (SDA) such as surfactant can easily composite with silica to produce the ordered nanostructures at the large area. By this method, the self-assembly film and nanostructural formation of chemical entities is at the basis of many biological or biomimetic processes and increasingly in the nanostructure materials syntheses.⁴ The self-assembled ionic and nonionic surfactants have been successfully utilized for preparing the ordered inorganic-organic hybrids with mesostructures as well as outstanding properties,⁵ and the hybrids have been employed for the biomedical applications.⁶ It is suggested that these hybrids can be widely applicable for the cell culture plates, contact lenses, and teeth and bone cements. However, the hybrids still have some problems of poor mechanical and viscoelastic properties such as high brittleness and low strength. They also react with the surrounding biological solutions and cells too fast *in vitro* and *in vivo*,⁷ which deteriorates their long-

term stability. Thus, the silica-surfactant hybrids with flexible and biocompatible chitosan (Chi) molecule,⁸ which is used as a commercial and low-cost biopolymer derived from the shells of crustaceans and the cell walls of fungi and yeast, as well as in squid pens,⁹ is one of the effective strategies for enhancing their mechanical properties as well as cytocompatibility. However, the Chi molecules exhibit the low compatibility with silicate materials because of the strong Chi self-aggregation force among the hydrophilic hydroxyl and α -glycoside groups in the molecular structure. Thus, it is proposed by this study that the segregated Chi nanostructures can be assisted by the surfactant-silica self-assemble process for the utilization.

In this study, the effective Chi-segregation nanodomains by the silica-surfactant hybrid film formation, which were synthesized based on a room-temperature sol-gel process using poly(ethylene oxide)-poly(propylene oxide)-poly(ethylene oxide) (PEO-PPO-PEO) triblock copolymer (TBC) as the SDA,^{5j} were prepared. The hybrid films with the different Chi concentrations were synthesized to clarify the additive effect of the Chi molecules on the self-assembly process at the film surface as shown in Fig. 1.

The synthetic process of the films followed the modified procedure from the previous reports.^{5h, 5j} 0.94 g of TBC (F127, PEO₁₀₆-PPO₇₀-PEO₁₀₆, Mw=12600) was dissolved in 6.8 mL of ethanol, and stirred. 2.0 mL of an hydrochloric acid aqueous solution (pH = 1.4) was added and stirred. Then, the Chi flakes (Funakosi Co. Ltd., Chitosan 7B KH001001) were added in the solution at the weight concentration of 0.0, 1.0, 5.0, 10 wt%. Then, 2.0 mL of tetraethylorthosilicate (TEOS) was added to the solution, and stirred at 40 °C for 2 h. The solution was transferred to Teflon vessels (bottom area: 7.9 cm²) at the density of 0.42 mL/cm², and stored for 3 days in order for allowing the gelation, and dried at 65 °C for 18 h. The films were peeled from the vessels and were abbreviated as **0w**-, **1w**-, **5w**- and **10w**-films prepared at the concentration of 0.0, 1.0, 5.0, 10 wt%, respectively.

The films were characterized by a UV-Visible spectrophotometer and X-ray diffraction (XRD) pattern. The total visible transmittance was calculated by averaging the values in the wavelength range between 400–800 nm. The surface nanostructures and viscoelastic properties were analysed by an atomic force microscope (AFM: Nanocute, SII Investments, Inc.) in areas of 0.5×0.5 and 1.0×1.0 μm^2 . The surface roughness (R_{rms}) was calculated by the root mean squares in the height images. The viscoelastic properties were calculated from the force curves, and the detailed measurement procedure was

^a Department of Materials Science and Technology, Nagaoka University of Technology, 1603-1 Kamitomioka, Nagaoka, Niigata 940-2188, Japan.

^b Top Runner Incubation Center for Academia-Industry Fusion, Nagaoka University of Technology, 1603-1 Kamitomioka, Nagaoka, Niigata 940-2188, Japan.

† Electronic Supplementary Information (ESI) available: [details of any supplementary information available should be included here]. See DOI: 10.1039/x0xx00000x

COMMUNICATION

described in the ESI, Experimental Procedure S1 and Scheme S1.

The osteoblast-like MC3T3-E1 cells were cultured in a cell culture flask containing 15 mL of the fetal bovine serum (FBS) dispersed in alpha-minimum essential medium (α MEM) at 10 vol% (10%FBS/ α MEM). The cells were incubated at 37 °C in a humidified atmosphere of CO₂, and subcultured every 7 days with trypsin-EDTA. After being washed with 15 mL of phosphate buffered saline (PBS) and treated with 1 mL of the trypsin-EDTA, the cells were dispersed in 15 mL of PBS and then in 15 mL of the 10%FBS/ α MEM. The number of cells in the suspension was seeded at the density of 3.0×10^3 cells·cm⁻² and then cultured for 36 h. After the culture, the cells were rinsed by PBS. Then, the cells adhered only on the film surfaces were characterized by a light-microscopy. The density and area of the adherent cell were counted and calculated from the 2-D images ($n = 50$). The cell viability with the culture time was measured as described in the ESI, Experimental Procedure S2 in detail. As compared to the reference, commercially-available tissue culture poly(styrene) (TCPS) was used. The statistical analysis was examined by the Student's *t* test.

The films with the different Chi concentrations were in a transparent and self-standing state with a length up to several centimetres (Fig. 1), whereas TEOS alone was in a fragmented state. The monolithic films have the thicknesses of several hundred micrometers (150–200 μ m), and the total transmittance is in the order of **0w**- (81 %T) > **1w**- (64 %T) > **5w**- (54 %T) > **10w**- (19 %T) films, and the Chi addition reduces the visible-light transmittance and scattering. The bending state photograph (**5w**-film) by the hand shown in Fig. 1

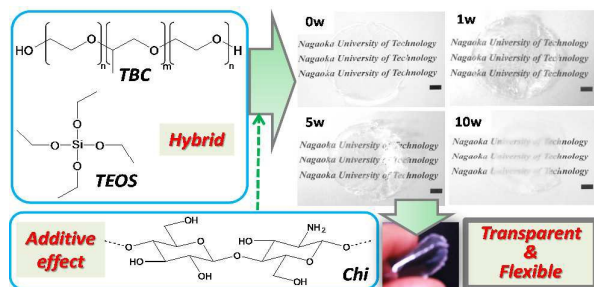


Fig. 1. Chemical structures of the reagents used in this study, and the photographs of the films with the different Chi concentrations (scale bar: 0.5 cm). (Lower photograph): the bending state of the **5w**-film, indicating the transparency and flexibility.

indicates the flexibility of the films. Therefore, the nanocomposite structures by the silica frameworks combined with the surfactant functional groups homogeneously stabilize the Chi molecules on the film surfaces.

Fig. 2 shows the AFM topographic and phase-shift images of the films at an observation area of $1 \times 1 \mu\text{m}^2$. The **0w**-film showed a nanoparticulate surface morphology that was flat surface structure at the R_{rms} value of 3.3 ± 1.9 nm. In contrast, the network fibrous nanostructures of Chi molecules were observed in the films containing Chi to be the R_{rms} values of 3.3 ± 1.3 nm, 3.4 ± 0.91 nm and 4.4 ± 2.2 nm for **1w**-, **5w**- and **10w**-films. Only by the Chi molecules cast on the **0w**-film after the silica-surfactant hybridization, the Chi molecules formed homogeneously-packed structures without nanostructures (ESI, Fig. S1). All the samples from the XRD patterns exhibited the broad patterns only from 100 plane ($d_{100} = 7.4$ – 7.6 nm) and the pattern shapes were almost same, which correspond to the

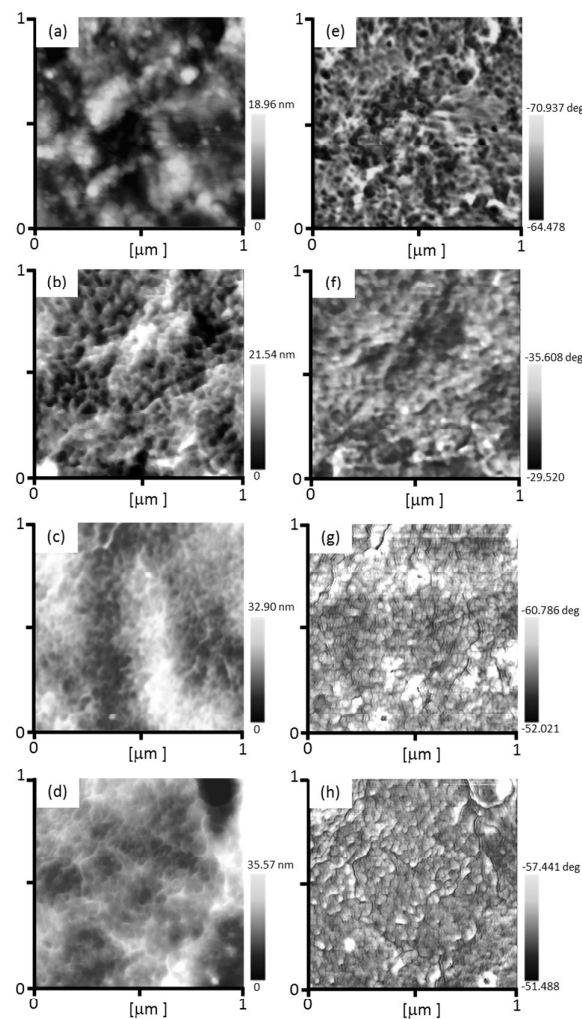


Fig. 2. AFM (a–d) topographic and (e–h) phase-shift images of (a, e) **0w**- (b, f) **1w**- (c, g) **5w**- and (d, h) **10w**-films with the different Chi concentrations in an observation area of $1.0 \times 1.0 \mu\text{m}^2$.

worm-like mesostructures of our previous report.^{5j} Therefore, the segregated nanofiber networks were successfully formed by the silica-surfactant nanocomposite process.

Fig. 3 (a–d) shows the force curves for the film surfaces. The five points measured for the force curves are marked in the AFM topographic images ($0.5 \times 0.5 \mu\text{m}^2$) in the ESI, Fig. S2. The typical tip-sample interactive behaviours were observed depending on the film surfaces. During the initial stage, there is a measurable attraction at the separation distance below 75 nm. A slight attractive force between the tip and the sample during the approaching process was observed, which is attributed to the interactions between the tip and surface molecules. This force strongly appears in the **0w**-film, suggesting that only the silica-surfactant composite strongly adsorbs on the SiO₂ probe tip surface.^{5j} Furthermore, the starting distance increased with increasing the Chi concentrations, suggesting the increase in the Chi segregation layer thickness.

A repulsion force between the tip and the sample is evident to exhibit the slopes, starting at the distance of around a few nanometers on **0w**- and **1w**-films and several tens nanometers on **5w**- and **10w**-films. This force is attributed to the overlap of the electric double layers around the two surfaces

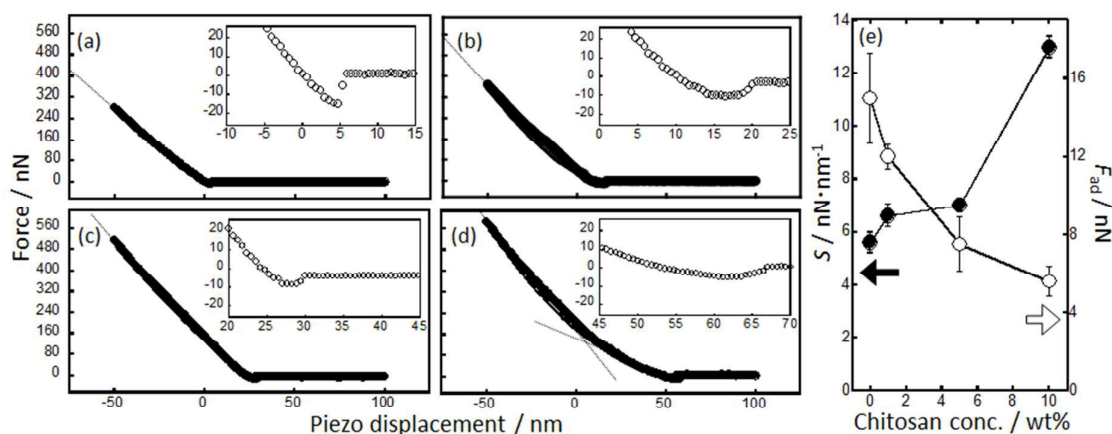


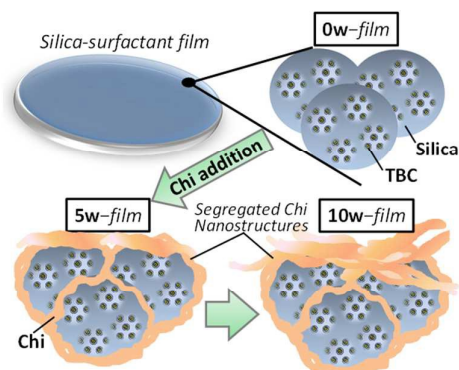
Fig. 3. Force curves (●: approaching, ○: retracting) of the (a) **0w**-, (b) **1w**-, (c) **5w**- and (d) **10w**-films. (Inset): the adhesive areas magnified in the retracting curves. (e): the S (close circles) and F_{ad} (open circles) value changes with the chitosan concentration. The dotted lines indicate the decline of the slopes. The calculation of the S and F_{ad} values were described in the ESI, Experimental Procedure S1 and Scheme S1.

between the tip and sample surfaces. The S (i.e., saturated slope) values of the film surfaces containing Chi (**1w**: 6.6 ± 0.43 , **5w**: 7.0 ± 0.21 , **10w**: 13.0 ± 0.41 nN/nm) are higher than that of the **0w**-film surface (5.6 ± 0.38 nN/nm) in Fig. 3 (e), and the **10w**-film surface is highest of all the surfaces, indicating the importance of the Chi segregation for the viscoelastic properties of the films. In particular, the **10w** film shows the two-step changes; the lower and higher S values would be attributed to the self-aggregation layer among Chi molecules and the Chi-silica-surfactant interactive layer, respectively, indicating the existence of the separated Chi layer. Furthermore, the E^* values of the films were 138 ± 9.5 , 165 ± 10 , 175 ± 5.3 and 325 ± 10.3 MPa for the **0w**-, **1w**-, **5w**- and **10w**-films, respectively.

At a separation distance in the retracting process, the tip jumps inward and subsequently a maximum F_{ad} was observed (Fig. 3 (a–d), Insets). It is reasonable to conclude that the film surfaces differently interacted with the fragmented surfaces after the insert of the tip, and the F_{ad} of the **0w**-film is the highest of all the surfaces, suggesting the favorable interactions (e.g., hydrogen bonding, electrostatic interactions) of the SiO_2 tip surfaces with sample surfaces of both the TBC and silica. In contrast, the segregated Chi nanofibers were difficult to interact with the tip surfaces due to the dominant self-aggregation among the Chi molecules.

In this study, the utilization of the insufficiency behaviour of natural products with the formation of siliceous compounds, which is thought to be scientific interest,¹² justifies the search for bioinspired synthesis, leading to novel silica-based hybrids with simple hierarchical structures or, at least, allowing the unique production under the soft-condition. In fact, inspired by nature, a variety of chemical reagents have been used to check *in vitro* silicification processes.¹³ In the material preparation, the additives (e.g., Chi), which intended to mimic active natural molecules, can play different roles: aggregation promoting reagents or SDA. In this study, the possible segregation mechanism was proposed as shown in Scheme 1. The Chi addition effectively induces the suitable segregation to form the nanofiber networks on the films, which were driven by the well-known silica-surfactant nanostructure formation based on the self-assembly process. As a result, the suitable segregation with the nanostructures was formed on the hybrids. Furthermore, this procedural approach will lead to bulk biosilica monolithic films or, alternatively, to similar highly-ordered mesoporous architectures when the SDA addition are well-controlled.

Fig. 4 (a–d) shows the light-microscope images of the cells adhered on the films. Taking into account the transparent and mechanical properties described above for the biomedical applications, **0w**-, **1w**- and **5w**-films were used in the following. The cells adhered on the films modified with Chi nanofibers clearly had the expanded fibrous pseudopods and show the anisotropic cellular morphologies (Fig. 4 (a, b)), whereas the cells on the **0w**-film and TCPS surfaces had the smaller isotropic morphologies. At the culture time of 36 h, the number of the expanded fibrous pseudopod per one cell was **5w** (7.8 ± 1.6 pieces/cell) > **1w** (5.5 ± 1.1 pieces/cell) > **0w** (5.1 ± 1.3 pieces/cell) > TCPS (5.2 ± 1.7 pieces/cell), suggesting the effective interfacial cell–film bindings at **5w**. As shown in Fig. 4 (c), the cell viability with the **0w**-film shows the lowest viability due to the influence of the hydrophilic PEO group. With increasing the Chi amount, the cell viability significantly increased. This indicated that the Chi molecules were functionalized on the surfaces to exhibit a good cytocompatibility, and **1w**- and **5w**-films showed the higher cell viability. Moreover, the density and area of the adherent cell are in the order of (**1w**, **5w**) > **0w** > TCPS (Fig. 4 (d, e)). Here, it has been reported that the cell survival was affected by the adherent cell shape.¹⁰ The osteoblast-like cells on Ta, Cr and hydroxyapatite had different adhesive areas,¹¹ suggesting that the difference in the surface properties affected the cell adhesive areas. With totally considering these results, the Chi segregation films (**1w**-, **5w**-films) of this study would provide a good cell activity and long cell survival. The different



Scheme 1. Possible scheme of the segregation states of Chi molecules on the silica-surfactant films.

COMMUNICATION

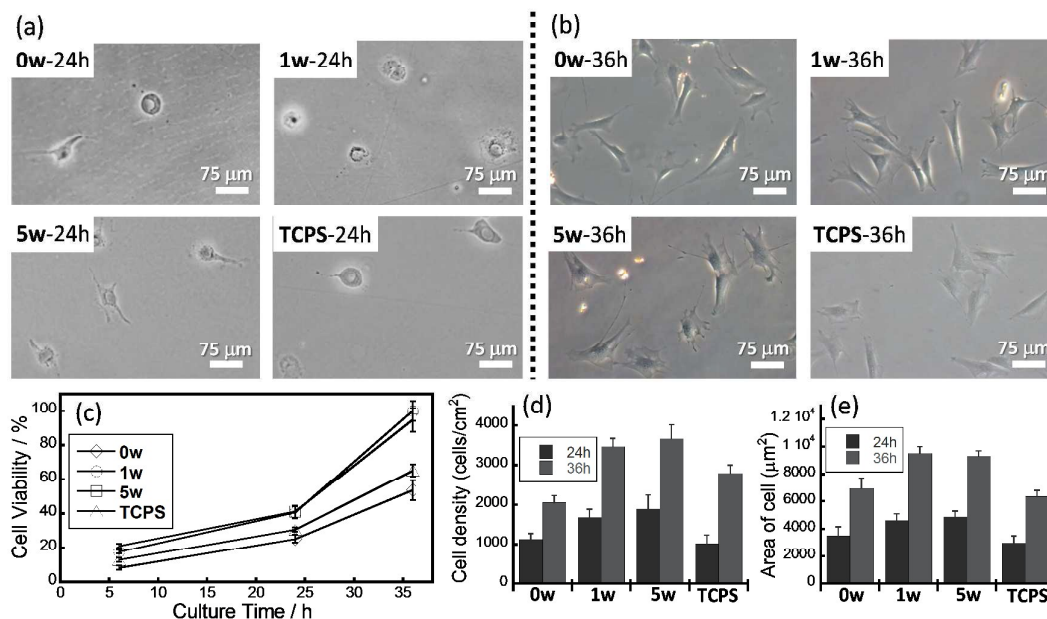


Fig. 4. Light-microscope images of the cells adhered on the 0w-, 1w- and 5w-films and TCPS at the culture times of (a) 24 h and (b) 36 h, and (c) the cell viability changes with the cell culture time, (d) density and (e) area of the cell.

structures would be attributed to the cell adhesion points with the sample surfaces, so that the cytoskeleton changes and extracellular matrix arrangements at the interfaces caused the binding behavior and morphologies.^{11c} Thus, the Chi nanostructures on the silica-TBC effectively promoted the osteoblast-like cell adhesion. The detailed nanostructural effect on the cell functions will be reported by our laboratory.

It has been reported that the bone healing process can be improved by controlling the composition and structure of the bone substitute nanomaterials composited with biocompatible polymers.¹⁴ The Chi nanocomposite film surfaces of this study significantly exhibited the higher cytocompatibility at the initial cell culture stage. Therefore, the recognition of cells on the Chi nanostructural surfaces caused the adhesion behaviors, and the interfacial viscoelastic layers by Chi nanofibers also effectively determined the cellular shapes (anisotropy or not) and functions, even though the pre-adsorbed protein states are important.^{11e}

Conclusions

The control of Chi segregation process by the surfactant-silica nanostructure formation was successfully achieved to clarify their self-assembled and rigid structures based on the interactions among the Chi molecules. The hierarchical Chi nanostructures provided the well-defined and extended nanodomains to resultantly be compatible with osteoblast-like cells.

Acknowledgements

This study was supported by a grant from the Japan Society for the Promotion of Science (JSPS) KAKENHI (Grant-in-Aid for Young Scientists (A), Grant No.: 26709052).

Notes and references

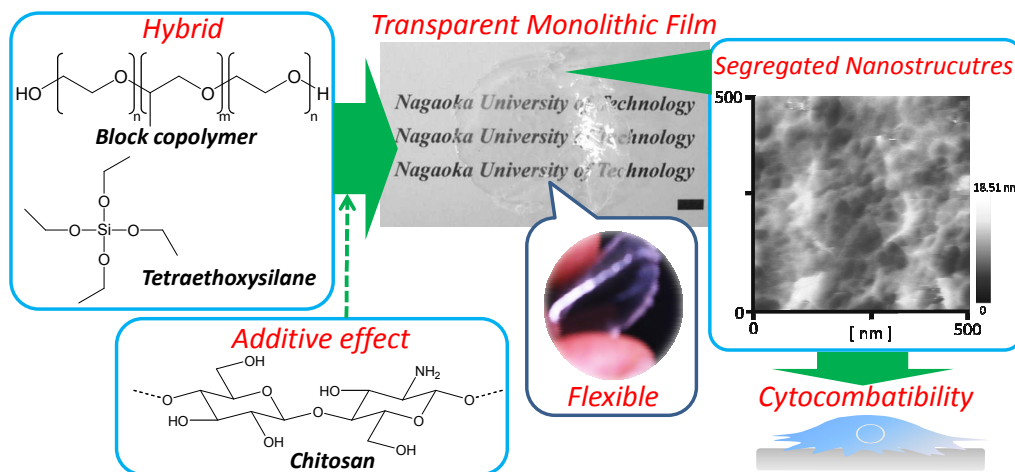
- (a) T. Coradin and J. Livage, *Acc. Chem. Res.*, 2007, **40**, 819; (b) M. Hildebran, *Chem. Rev.*, 2008, **108**, 4855.
- (a) B. Kasemo, *Surf. Sci.*, 2002, **500**, 656; (b) M. Arnold, E. A. Cavalcanti-Adam, R. Glass, J. Bluemmel, W. Eck, M. Kantelehner, H. Kessler and J. P. Spatz, *Chem. Phys. Chem.*, 2004, **5**, 383; (c) K. Kang, S.-E. Choi, H. S. Jang, W. K. Cho, Y. Nam, I. S. Choi, J. S. Lee,

Angew. Chem. Int. Ed. 2012, **124**, 2909; (d) K. Kang, S. Y. Yoon, S.-E. Choi, M.-H. Kim, M. Park, Y. Nam, J. S. Lee, I. S. Choi, *Angew. Chem. Int. Ed.* 2014, **53**, 6075. (e) K. L. Tovar-Carrillo, S. S. Sueyoshi, M. Tagaya and T. Kobayashi, *Indust. Eng. Chem. Res.*, 2013, **52**, 11607; (f) K. L. Tovar-Carrillo, M. Tagaya and T. Kobayashi, *Indust. Eng. Chem. Res.*, 2014, **53**, 4650.

- (a) Y. Cho and A. Ivanisevic, *J. Phys. Chem., B*, 2004, **108**, 15223; (b) J.D. Hoff, L.J. Cheng, E. Meyhöfer, L.J. Guo and A.J. Hunt, *Nano Lett.*, 2004, **4**, 853; (c) A. Monkawa, T. Ikoma, S. Yunoki, K. Ohta and J. Tanaka, *Mater. Lett.*, 2006, **60**, 3647; (d) M. Okuda, M. Takeguchi, M. Tagaya, T. Tonegawa, A. Hashimoto, N. Hanagata and T. Ikoma, *Micron*, 2009, **40**, 665; (e) M. Okuda, N. Ogawa, M. Takeguchi, A. Hashimoto, M. Tagaya, S. Chen, N. Hanagata and T. Ikoma, *Micros. Microanal.*, 2011, **17**, 788; (f) M. Tagaya, Y. Hoshina, N. Ogawa, M. Takeguchi and T. Kobayashi, *Micron*, 2013, **46**, 22.
- (a) G. M. Whitesides and B. Grzybowski, *Science*, 2002, **295**, 2418; (b) I. W. Hamley, *Angew. Chem.*, 2003, **115**, 1730; (c) S. Mann, *Nat. Mater.*, 2009, **8**, 781; (d) V. Puchol, J. El Haskouri, J. Latorre, C. Guillem, A. Beltrán, D. Beltrán and P. Amorós, *Chem. Commun.*, 2009, **19**, 2694. (e) B. Alonso and E. Belamie, *Angew. Chem. Int. Ed.*, 2010, **49**, 8201; (f) C. Dai, C. Liu, J. Wei, H. Hong and Q. Zhao, *Biomater.*, 2010, **31**, 7620.
- (a) T. Yanagisawa, T. Shimizu, K. Kuroda and C. Kato, *Bull. Chem. Soc. Jpn.*, 1990, **63**, 988; (b) C. T. Kresge, M. E. Leonowicz, W. J. Roth, J. C. Vartuli and J. S. Beck, *Nature*, 1992, **359**, 710; (c) D. Y. Zhao, J. L. Feng, Q. S. Huo, N. Melosh, G. H. Fredrickson, B. F. Chmelka and G. D. Stucky, *Science*, 1998, **279**, 548; (d) A. Corma, *Chem. Rev.*, 1997, **97**, 2373; (e) M. E. Davis, *Nature*, 2002, **417**, 813; (f) K. B. Yoon, *Chem. Rev.*, 1993, **93**, 321; (g) K. Moller and T. Bein, *Chem. Mater.*, 1998, **10**, 2950; (h) N. A. Melosh, P. Lipic, F. S. Bates, F. Wudl, G. D. Stucky, G. H. Fredrickson and B. F. Chmelka, *Macromolecules* 1999, **32**, 4332; (i) A. Stein, B. J. Melde and R. C. Schroden, *Adv. Mater.*, 2000, **12**, 1403; (j) M. Tagaya, N. Hanagata and T. Kobayashi *ACS Appl. Mater. Interf.*, 2012, **4**, 6169.
- (a) M. Tagaya and M. Ogaawa, *Chem. Lett.*, 2006, **35**, 108; (b) M. Tagaya and M. Ogawa, *Phys. Chem. Chem. Phys.*, 2008, **10**, 6849; (c) M. Okuda, M. Takeguchi, Y. Zhu, A. Hashimoto, N. Ogawa, M. Tagaya, S. Chen, N. Hanagata and T. Ikoma, *Surf. Interface Anal.*, 2010, **42**, 1548; (d) M. Tagaya, T. Ikoma, T. Yoshioka, T. Motozuka, F. Minami and J. Tanaka, *Mater. Lett.*, 2011, **65**, 2287; (e) M. Tagaya, T. Ikoma, T. Yoshioka and J. Tanaka, *J. Colloid Interface Sci.*, 2011, **363**, 456; (f) M. Tagaya, T. Ikoma, T. Yoshioka and J. Tanaka, *Chem. Commun.*, 2011, **47**, 8430; (g) M. Tagaya, S. Motozuka, T. Kobayashi,

- T. Ikoma, J. Tanaka, *J. Mater. Chem.*, 2012, **22**, 18741.
7. (a) E. Nilsen, M. A. Einarsrud and G. W. Scherer, *J. Non-Cryst. Solids.*, 1997, **221**, 135; (b) D. Avnir, T. Coradin, O. Lev and J. Livage, *J. Mater. Chem.* 2006, **16**, 1013.
 8. (a) A. D. Martino, M. Sittinger and M. V. Risbud, *Biomater.*, 2005, **26**, 5983; (b) H. Ueno, H. Yamada, I. Tanaka, N. Kaba, M. Matsuura, M. Okumura, T. Kadosawa and T. Fujinaga, *Biomater.*, 1999, **20**, 1407.
 9. G. F. Payne and S. R. Raghavan, *Soft Matter.*, 2007, **3**, 521.
 10. C. S. Chen, M. Mrksich, S. Huang, G. M. Whitesides and D. E. Ingber, *Science*, 1997, **5317**, 1425.
 11. (a) C. Modin, A. L. Stranne, M. Foss, M. Duch, J. Justesen, J. Chevallier, L. K. Andersen, A. G. Hemmersam, F. S. Pedersen and F. Besenbacher, *Biomater.*, 2006, **27**, 1346; (b) M. Tagaya, T. Ikoma, T. Takemura, N. Hanagata, M. Okuda, T. Yoshioka and J. Tanaka, *Langmuir*, 2011, **27**, 7635; (c) M. Tagaya, T. Ikoma, T. Takemura, N. Hanagata, and J. Tanaka, *Langmuir*, 2011, **27**, 7645.
 12. (a) R. L. Brutchey and D. E. Morse, *Chem. Rev.*, 2008, **108**, 4915; (b) C. Sanchez, H. Arribart and M. M. G. Guille, *Nat. Mater.*, 2005, **4**, 277.
 13. (a) S. V. Patwardhan, S. J. Clarson and C. C. Perry, *Chem. Commun.*, 2005, 1113; (b) A. Corma, M. J. Díaz-Cabañas, M. Moliner and G. Rodriguez., *Chem. Commun.*, 2006, 3137.
 14. (a) K. Vassilis and K. David, *Biomaterials*. 2005, **26**, 5474; (b) A. G. A. Coombes and M. C. Meikle, *Clin. Mater.*, 1994, **17**, 35; (c) E. J. Lee, S. H. Jun, H. E. Kim, H. W. Kim, Y. H. Koh and J. H. Jang, *J. Mater. Sci.: Mater. Med.*, 2010, **21**, 207.

Visual Abstract



The segregation nanostructures of Chi molecules by a silica-surfactant self-assemble film formation process were successfully prepared, and their self-organization effectively affects the cytocompatibility.